

# A NOVEL FULLY COUPLED GEOMECHANICAL MODEL FOR CO<sub>2</sub> SEQUESTRATION IN FRACTURED AND POROUS BRINE AQUIFERS

Philip H. Winterfeld\* and Yu-Shu Wu†

\*.†Colorado School of Mines  
Department of Petroleum Engineering  
1613 Illinois St., Golden, CO 80401 USA  
\*e-mail: pwinterf@mines.edu  
†e-mail: ywu@mines.edu

**Key words:** Reservoir simulator, thermal-hydrologic-mechanical, fully coupled, CO<sub>2</sub> sequestration

## 1 INTRODUCTION

Numerical simulation of thermal-hydrologic-mechanical (THM) processes in fractured and porous media can be applied to solving practical problems in many areas including CO<sub>2</sub> sequestration in saline aquifers. THM simulators are based on Darcy's law for multiphase flow with conservation of mass, Biot's theory of poroelasticity (extended to fractured media) with conservation of momentum, and Fourier's law of heat conduction with conservation of energy. One approach to simulating THM processes in reservoirs<sup>1</sup> is fully coupled, where flow (pore pressure and saturations) and geomechanical variables (stresses and displacements), and temperature are solved simultaneously. This approach was taken by Chin et al.<sup>2</sup> and Osario et al.<sup>3</sup>, but both formulations were isothermal and single phase.

This paper presents a fully coupled, fully implicit THM simulator. The geomechanical equations relating stresses and displacements are combined to yield an equation for mean stress as a function of pore pressure and temperature. The multiphase and heat flow formulation is that for TOUGH2<sup>4</sup>, the starting point for our simulator, and we add the mean stress equation (with mean stress as an additional primary variable) to that formulation. In addition, theories of poroelasticity<sup>5,6</sup> and experimental studies<sup>7,8</sup> have correlated porosity and permeability to effective stress (the difference between mean stress and pore pressure); we incorporate those dependencies into our simulator as well.

The simulator formulation and numerical implementation are verified using analytical solutions and example problems from the literature. We simulated a double porosity one-dimensional consolidation problem that has an analytical solution. Problems from the literature include simulation of CO<sub>2</sub> sequestration in a hypothetical aquifer-caprock system and CO<sub>2</sub> storage in a gas field.

## 2 TOUGH2 SIMULATORS

Our simulator is a modification of TOUGH2-MP<sup>9</sup>, a massively parallel version of TOUGH2. TOUGH2 is a well known numerical simulator of multi-component, multiphase fluid and heat flow in porous and fractured media. TOUGH2 was designed primarily for applications in geothermal reservoir engineering, nuclear waste disposal, and environmental assessment and remediation. In the TOUGH2 formulation, fluid advection is described with a multiphase extension of Darcy's law and there is diffusive mass transport in all phases. Heat flow occurs by conduction and convection, and includes sensible as well as latent heat effects. Phases are in local equilibrium. TOUGH2 solves mass and energy balances over the simulation domain using the integral finite difference method<sup>10</sup> on an unstructured grid.

The TOUGH2 family of codes consists of functional units, such as a grid generator and a physical property module, with flexible and transparent interfaces. The physical property module ECO2N<sup>11</sup> was designed for CO<sub>2</sub> sequestration in saline aquifers. It includes a description of the relevant properties of H<sub>2</sub>O–NaCl–CO<sub>2</sub> mixtures that is highly accurate for the temperature, pore pressure, and salinity conditions of interest (between 10 and 110 °C, pore pressure less than 600 bar, and salinity up to full halite saturation). An aqueous and a CO<sub>2</sub>-rich phase may be present, and salt may be present in the aqueous phase or as a solid precipitate. It can model super- and sub-critical conditions, but does not distinguish between liquid and gaseous CO<sub>2</sub>.

### 3 MEAN STRESS EQUATION

We derive the governing equation for mean stress in this section. The stress-strain relationship for an elastic fluid-filled porous media under non-isothermal conditions is<sup>12</sup>

$$\bar{\tau} - (\alpha P + 3\beta K(T - T_{\text{ref}}))\bar{\mathbb{I}} = 2G\bar{\epsilon} + \lambda(\text{tr}\bar{\epsilon})\bar{\mathbb{I}} \quad (1)$$

where  $T_{\text{ref}}$  is reference temperature,  $\beta$  is linear thermal expansion coefficient,  $K$  is bulk modulus,  $G$  is shear modulus,  $\lambda$  is the Lamé parameter, and  $\alpha$  is the Biot coefficient. Two terms are subtracted from the normal stress tensor components in this thermo-poroelastic extension of Hooke's law. The first is the pore pressure term from poroelasticity theory and the second is the temperature term from thermo-elasticity theory. We obtain the multi-porosity generalization of Equation 7 from Bai et al.<sup>13</sup> while retaining the temperature term from Equation 1

$$\bar{\tau} - \left( \sum \alpha_k P_k + 3\beta K(T_k - T_{\text{ref}}) \right) \bar{\mathbb{I}} = 2G\bar{\epsilon} + \lambda(\text{tr}\bar{\epsilon})\bar{\mathbb{I}} \quad (2)$$

where the subscript  $k$  refers to the porous continuum ( fracture or matrix for double-porosity systems). Expressions for the generalized Biot coefficients  $\alpha_k$  for a double-porosity medium have been presented by Wilson and Aifantis<sup>14</sup>

$$\begin{aligned} \alpha_1 &= 1 - \frac{K}{K_*} \\ \alpha_2 &= \frac{K}{K_*} \left( 1 - \frac{K_*}{K_S} \right) \end{aligned} \quad (3)$$

where  $K_s$  is the solid modulus,  $K_*$  is the modulus of the porous medium without the fractures, subscript 1 refers to the fractures, and subscript 2 to the matrix.

We obtain a relationship between volumetric strain,  $\epsilon_v$ , and mean stress,  $\tau_m$ , by taking the trace of Equation 2

$$K\epsilon_v = \tau_m - \sum \alpha_k P_k - 3\beta K(T_k - T_{ref}) \quad (4)$$

The strain tensor and the displacement vector  $\bar{u}$  are related by

$$\bar{\epsilon} = \frac{1}{2} (\nabla \bar{u} + \nabla \bar{u}^t) \quad (5)$$

and the static equilibrium equation is

$$\nabla \cdot \bar{\tau} + \bar{F} = 0 \quad (6)$$

where  $\bar{F}$  is the body force. We combine Equations 2, 5, and 6 to obtain the thermo-poroelastic Navier equations for a multi-porosity medium

$$\nabla \left( \sum \alpha_k P_k + 3\beta K T_k \right) + (\lambda + G) \nabla (\nabla \cdot \bar{u}) + G \nabla^2 \bar{u} + \bar{F} = 0 \quad (7)$$

Taking the divergence of Equation 7, noting the divergence of the displacement vector is the volumetric strain, and combining with Equation 4 yields the governing equation for mean stress

$$\frac{3(1-\nu)}{1+\nu} \nabla^2 \tau_m + \nabla \cdot \bar{F} - \frac{2(1-2\nu)}{1+\nu} \nabla^2 \left( \sum \alpha_k P_k + 3\beta K T_k \right) = 0 \quad (8)$$

where  $\nu$  is Poisson's ratio.

#### 4 ROCK PROPERTY CORRELATIONS

Correlations have been developed for porosity as a function of effective stress and permeability as a function of porosity. A theory of hydrostatic poroelasticity<sup>15</sup> has been proposed that accounts for the coupling of rock deformation with fluid flow inside the porous rock. Porosity as a function of effective stress is derived from this theory

$$d\phi = - \left[ \frac{1}{K} (1 - \phi) - C_r \right] d\tau' \quad (9)$$

where  $\tau'$  is effective stress and  $C_r$  is rock grain compressibility.

Porosity is the ratio of fluid to bulk (solid plus fluid) volume. Bulk volume,  $V$ , is related to volumetric strain by

$$V = V_0 (1 - \epsilon_v) = V_i \frac{(1 - \epsilon_v)}{(1 - \epsilon_{v,i})} \quad (10)$$

where  $V_0$  is zero strain volume and subscript  $i$  refers to reference conditions. Gutierrez<sup>16</sup> presented expressions for solid volume change with pore pressure and effective stress, which combined with the above yield the following expression for porosity

$$\phi = 1 - \frac{(1 - \phi_i)V_i + \frac{(1 - \phi_i)}{K_s}(P - P_i) - \frac{1}{K_s}(\tau' - \tau'_i)}{V_i \frac{(1 - \epsilon_v)}{(1 - \epsilon_{v,i})}} \quad (11)$$

Rutqvist et al.<sup>17</sup> presented the following function for porosity, obtained from laboratory experiments on sedimentary rock<sup>18</sup>

$$\phi = \phi_r + (\phi_0 - \phi_r)e^{-a\tau'} \quad (12)$$

where  $\phi_0$  is zero effective stress porosity,  $\phi_r$  is high effective stress porosity, and the exponent  $a$  is a parameter. They also presented an associated function for permeability in terms of porosity

$$k = k_0 e^{c\left(\frac{\phi}{\phi_0} - 1\right)} \quad (13)$$

Ostensen<sup>19</sup> studied the relationship between effective stress and permeability for tight gas sands and approximated permeability as

$$k^n = D \ln \frac{\tau'^*}{\tau'} \quad (14)$$

where exponential  $n$  is 0.5,  $D$  is a parameter, and  $\tau'^*$  is effective stress for zero permeability, obtained by extrapolating permeability versus effective stress on a semi-log plot.

Verma and Pruess<sup>20</sup> presented a power law expression relating permeability to porosity

$$\frac{k - k_c}{k_0 - k_c} = \left( \frac{\phi - \phi_c}{\phi_0 - \phi_c} \right)^n \quad (15)$$

where  $k_c$  and  $\phi_c$  are asymptotic values of permeability and porosity, respectively, and exponent  $n$  is a parameter.

The above correlations for porosity and permeability as a function of effective stress have been incorporated into our simulator.

## 5 EXAMPLE SIMULATIONS AND DISCUSSION

We describe several simulations to provide model verification and application examples. The first, one-dimensional consolidation of a double porosity medium is compared to an analytical solution. This is followed by CO<sub>2</sub> sequestration in a hypothetical aquifer-caprock system, including pressure response, surface uplift, and the effect of a fractured zone in the caprock. Finally, we simulate CO<sub>2</sub> storage in a gas field.

## 5.1 One-Dimensional Consolidation of Double Porosity Medium

Consider a fluid filled, double porosity one-dimensional column with a rigid impermeable

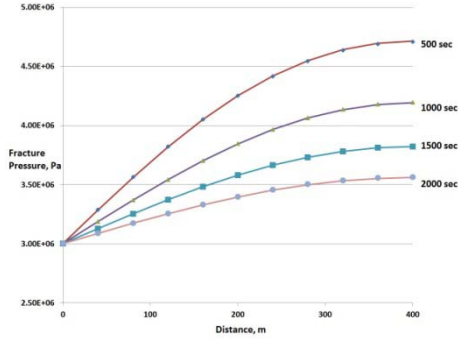


Figure 1. Comparison of analytical solution (solid lines) to simulation (points) for one-dimensional consolidation.

base and a top that is permeable to fluid. A constant load is applied to the top, causing an instantaneous, undrained pressurization of the column. Subsequently, fluid drains through the top until equilibrium is reached. An analytical solution to this problem was presented by Wilson and Aifantis<sup>14</sup> and includes expressions for fracture and matrix pressure. We ran this problem on our code for a 400 m column subdivided into 10,000 grid blocks with equilibrium pressure of  $3 \cdot 10^6$  Pa and undrained pressurization by the applied load of  $5.1 \cdot 10^6$  Pa. Figure 7 compares simulated fracture pressure to the analytical solution. Agreement between the two is excellent.

## 5.2 CO<sub>2</sub> Sequestration in an Aquifer-Caprock System

Rutqvist and Tsang<sup>21</sup> simulated CO<sub>2</sub> injection into a hypothetical aquifer-caprock system to study CO<sub>2</sub> plume spread, ground surface uplift, the possibility of mechanical failure, and other changes induced by the injection. The system consisted of a 200 m thick aquifer bounded below by a 1500 m thick base rock and above by 100 m caprock and a 1200 m zone that extends to the surface. CO<sub>2</sub> was injected at a constant rate at the aquifer bottom for ten years. They simulated this system using the coupled TOUGH2-FLAC simulator, with TOUGH2 handling multiphase flow and heat transport and FLAC handling rock deformation. We reran their case of homogeneous caprock without fractures, using effective stress dependent porosity and permeability (Eqns. 12 and 13). Figures 2 and 3 compare CO<sub>2</sub> saturation profiles after ten years injection, with quantitative similarity.

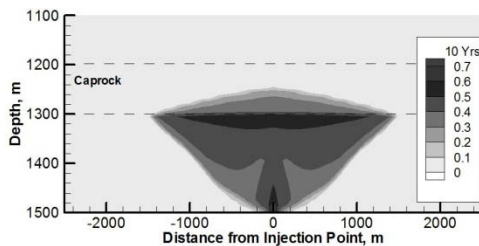


Figure 2. CO<sub>2</sub> saturation profile at ten years.

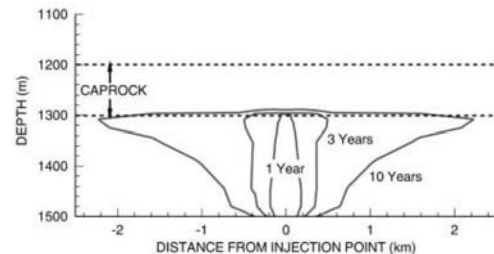


Figure 3. Rutqvist and Tsang<sup>21</sup> CO<sub>2</sub> saturation.

CO<sub>2</sub> injection increases the pore pressure, resulting in changes to mean stress and volumetric strain. Ground surface uplift is calculated from volumetric strain changes by summation over z-direction grid block columns and the assumption of strain isotropy. Figures 4 and 5 compare surface uplift at various times. These simulations show similar surface uplift profiles.

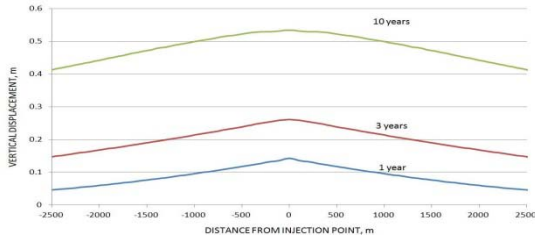


Figure 4. Surface uplift at 1, 3, and 10 years.

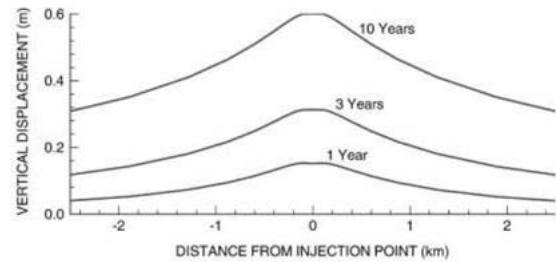


Figure 5. Rutqvist and Tsang<sup>21</sup> surface uplift.

Rutqvist and Tsang<sup>21</sup> also studied the effects of a vertical fracture zone in the caprock above the aquifer. We simulated this fracture zone by treating a column of grid blocks spanning the caprock zone as double porosity (fracture and matrix) with the rest of the grid being single porosity. Figures 6 and 7 compare CO<sub>2</sub> saturation profiles after ten years injection, again with quantitative similarity.

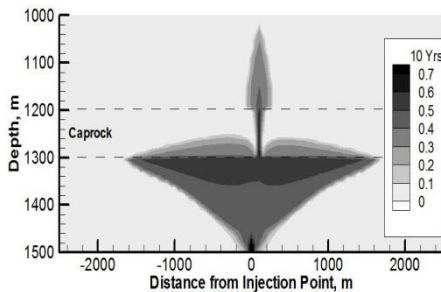


Figure 6. CO<sub>2</sub> saturation profile at 10 years with fracture zone.

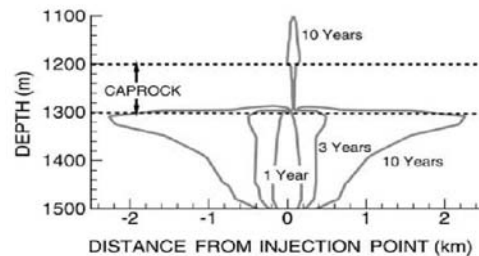


Figure 7. Rutqvist and Tsang<sup>21</sup> CO<sub>2</sub> saturation profile.

### 5.3 In Salah Project Simulation

The In Salah Gas Project, located in central Algeria, is a CO<sub>2</sub> storage project. Natural gas produced nearby is high in CO<sub>2</sub> and this CO<sub>2</sub> is injected back into the water leg of a depleting gas field for geological storage. Surface uplift from CO<sub>2</sub> injection has been measured by satellite-based interferometry and Rutqvist et al.<sup>22</sup> did a reservoir-geomechanical analysis of In Salah CO<sub>2</sub> injection and surface uplift using the TOUGH2-FLAC numerical simulator in order to determine if the uplift can be explained by pressure changes and deformation in the injection zone

only. We reran their analysis on our code, and we used a cluster computer to demonstrate our parallel code's ability to simulate larger problems.

The simulated domain was 10x10x4 km with one 1.5 km horizontal injection well at 1810 m depth and in the domain center. The domain consisted of four geological layers, Shallow Overburden, Caprock, Injection Zone, and Base, all with constant properties. CO<sub>2</sub> was injected for three years at 13.6 kg/sec. We simulated a 5x5x4 km quarter symmetry element of their system with a 400x400x60 grid (9.6 million grid blocks). Figure 8 shows surface uplift, calculated by assuming strain isotropy, after three years of CO<sub>2</sub> injection and Figure 9 is a comparison of surface uplift at the well's center versus depth to that of the reference.

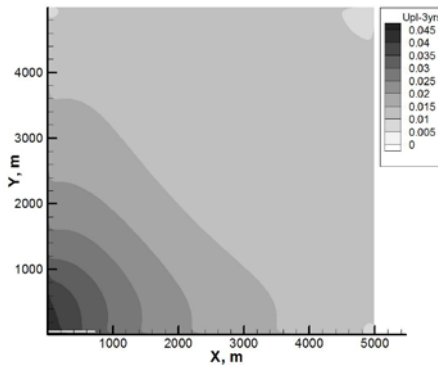


Figure 8. Surface uplift for quarter symmetry element. Injection well shown by thick horizontal line at origin.

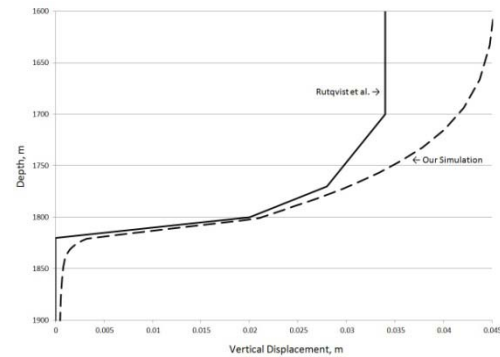


Figure 9. Comparison of surface uplift versus depth at well center.

## 6 CONCLUSIONS

We have developed a massively parallel reservoir simulator for modeling THM processes associated with CO<sub>2</sub> sequestration in fractured and porous media aquifers. We derived, from the fundamental equations describing deformation of porous and fractured elastic media, a conservation equation relating mean stress, pore pressure, and temperature, and incorporated it alongside the mass and energy conservation equations of TOUGH2-MP, the starting point for the simulator. In addition, rock properties, namely permeability and porosity, are functions of pore pressure and effective stress that are obtained from the literature.

We verified the simulator formulation and numerical implementation using an analytical solution to one-dimensional consolidation of a double porosity medium. We compared our results to those from two coupled computer codes, one that simulates fluid flow and heat transport, and another that simulates rock deformation. We obtained a good match of surface uplift and CO<sub>2</sub> profiles for injection into a caprock-aquifer system, CO<sub>2</sub> profiles for injection into the same system with a fractured zone in the caprock, and surface uplift occurring during CO<sub>2</sub> storage. This agreement indicates that our formulation is able to capture THM effects modeled by a coupled simulation with a more detailed handling of rock mechanics.

## ACKNOWLEDGEMENTS

This work was supported by the CMG Foundation and by the Assistant Secretary for Fossil Energy, Office of Coal and Power R&D through the National Energy Technology Laboratory under U.S. Department of Energy Contract Number DE-FC26-09FE0000988.

## REFERENCES

- [1] Mainguy M, Longuemare P. Coupling fluid flow and rock mechanics formulations of the partial coupling between reservoir and geomechanics simulators. *Oil Gas Sci Tech* 2002; 57: 355–67.
- [2] Chin LY, Raghavan R, Thomas LK. Fully coupled geomechanics and fluid-flow analysis of wells with stress-dependent permeability. *SPE Journal* March 2000; 5,1:32-45.
- [3] Osorio JG, Chen HY, Teufel L, Schaffer S. A two-domain fully coupled fluid-flow/geomechanical simulation model for reservoirs with stress-sensitive mechanical and fluid-flow properties. *SPE/ISRM Eurock'98*, Norway, July 8-10, 1998; 455-64.
- [4] Pruess K. TOUGH2—a general purpose numerical simulator for multiphase fluid and heat flow. Lawrence Berkeley National Laboratory Report LBL-29400, 1991.
- [5] Geertsma J. The effect of fluid pressure decline on volumetric changes of porous rock. *Trans AIME* 1957; 210:331-9.
- [6] Zimmerman RW. *Compressibility of sandstones*. Amsterdam: Elsevier; 1991.
- [7] Nur A, Byerlee JD. An exact effective stress law for elastic deformation of rock with fluids. *J Geophys Res* 1971; 76:6414-9.
- [8] Gobran BD, Brigham WE, Ramey HJ Jr. Absolute permeability as a function of confining pressure, pore pressure, and temperature. *SPE Formation Evaluation* March 1987; 77-84.
- [9] Zhang K, Wu YS, Pruess K. User's guide for TOUGH2-MP - a massively parallel version of the TOUGH2 code. Lawrence Berkeley National Laboratory Report LBNL-315E, 2008.
- [10] Narashimhan TN, Witherspoon PA. An integrated finite difference method for analysis of fluid flow in porous media. *Water Resour Res* 1976;1257–64.
- [11] Pruess K, Spycher N. ECO2N – a fluid property module for the TOUGH2 code for studies of CO<sub>2</sub> storage in saline aquifers. *Energy Conversion and Management* 2007; 48:1761-7.
- [12] McTigue DF. Thermoelastic response of fluid-saturated porous rock. *Journal of Geophysical Research*, August 10 1986; 91,9:9533-42.
- [13] Bai M, Elsworth D, Roegiers J-C. Modeling of naturally fractured reservoirs using deformation dependent flow mechanism. *Int. J. Rock Mech. Min. Sci. and Geomech. Abstr.* 1993, Vol. 30, No. 7, 1185-1191.
- [14] Wilson RK, Aifantis, EC. On the theory of consolidation with double porosity. *Int. J. Eng. Sci.* 1982, V 20, No 9, 1009-35.
- [15] Zimmerman RW, Somerton WH, King MS. Compressibility of porous rocks. *J Geophys Res* 1986; 91,12:765–77.
- [16] Gutierrez M, Lewis RW. Petroleum reservoir simulation coupling fluid flow and geomechanics. *SPE Reservoir Evaluation & Engineering*, June 2001; 164-72.
- [17] Rutqvist J, Wu YS, Tsang CF, Bodvarsson GA. Modeling approach for analysis of coupled multiphase fluid flow heat transfer and deformation in fractured porous rock. *Int J Rock Mech Min Sci* 2002; 39:429–42.
- [18] Davies JP, Davies DK. Stress-dependent permeability characterization and modeling. Paper SPE 56813. Presented at SPE ATCE, Houston, TX, October 1999.
- [19] Ostensen RW. The effect of stress-dependent permeability on gas production and well testing. *SPE Form Eval*, June 1986; 227–35.
- [20] Verma A, Pruess K. Thermohydrological conditions and silica redistribution near high-level nuclear wastes emplaced in saturated geological formations. *J Geophys Res* 1988; 93:1159-73.
- [21] Rutqvist J, Tsang, C-F. A study of caprock hydromechanical changes associated with CO<sub>2</sub>-injection into a brine formation. *Environmental Geology* 2002 42:296–305
- [22] Rutqvist J, Vasco DW, Myer L. Coupled reservoir-geomechanical analysis of CO<sub>2</sub> injection and ground deformations at In Salah Algeria. *Int. J. of Greenhouse Gas Control* 2010; 4:225–30.